

Crushing Force Theoretical Examination in One Cone Inertial Crusher

Simeon Savov

Dept. of Mining Mechanisation
Faculty of Mining
Electromechanics
University of Mining and
Geology "St. Ivan Rilski"
Sofia, Bulgaria
e-mail: ss.ss@abv.bg

Petko Nedyalkov

Dept. of Machine Elements and
Non-metallic Constructions
Faculty of Mechanical
Engineering
Technical University of Sofia
Sofia, Bulgaria
e-mail: nedpetko@tu-sofia.bg

Ivan Minin

Dept. of Mining Mechanisation
Faculty of Mining
Electromechanics
University of Mining and
Geology "St. Ivan Rilski"
Sofia, Bulgaria
e-mail: minin@dir.bg

Abstract—Cone inertial crushers are dynamical machine operating with centrifugal vibrator acting over the crushing cones of the crusher, typically operating with strong brittle materials, with wide adjusting possibilities of working regimes which gave broad particle sizes, forms and productivity. The aim of this paper is to look inside the crushing chamber and examines the inner relations of cone geometry parameters, inertia parameters, force, kinematic and dynamic relations in theoretical review compared with real limitations of machine parameters taken from experimental research. The presented investigation develops the comprehension of significance and importance in difference valuation of inner cone precession speed and angular speed of provoking body centrifugal vibrator.

Keywords—Cone Inertial Crusher; Kinematic and Dynamic relations; Inner Cone; Precession Speed; Angular Speed; Centrifugal Vibrator

I. INTRODUCTION

Cone inertial crushers (KID) are dynamical machine operating with centrifugal vibrator acting over the crushing cones of the crusher. As it is accepted from their principle of operation, they can operate with strong brittle materials, and it is possible to adjust the working regimes in terms of regulation the centrifugal force and discharging hole, which will lead to different size of product and different productivity.

The aim of this paper is to jump inside the crushing chamber and examines the inner relations of cone geometry parameters, inertia parameters, kinematic and dynamic relations. Theoretical investigations in closed crushing chamber always faces at some obstacles, so there are presented the idealizations, approximations and some assumptions helping that research.

Regarding previous researchers [1, 2, 3, 6] the presented investigation develop the comprehension of significance and importance in difference valuation of inner cone precession speed and angular speed of provoking body - centrifugal vibrator.

The schematically setup of machine is described via Fig. 1, where the inner cone (1) is supported with spherical bearing (4) over the outer cone – housing

(2). The centrifugal vibrator (3) is supported with cylindrical bearing (5) over the inner cone shaft. Static discharge hole output is mentioned with b (mm) and resulting dynamical movement of the cone is shown with S_0 (mm). Crushing chamber is formed between the outer cone (2) and inner cone (1). Supports of the outer cone are presented with spring elements (6).

II. METHODOLOGY FOR DETERMINING CURSHING FORCE

Spatial dynamics of 3D bodies with acting over them dynamical forces is quite a complicated problem, so with an acceptance of some engineering mistake it is possible to assume some idealizations of theoretical calculation for crushing force of examined cone inertial crusher. The idealizations that are used in presented paper follows:

- Full symmetric relationship between horizontal inertia axis of the machine, that allow to examine planar force and movement layout.
- Small resulting displacement gave possibility to accept that arcs of movement can be accepted as line segments.
- Small resulting displacements gave possibility to accept that components of movement, movement speed and angular speed in direction that is not coincident with main rotation and precession axis are neglectible.
- Direction of the equivalent crushing force is perpendicular to the crushing surface (as it is similar to classical cone crusher [4]).

The planar layout of forces acting over the inner cone [5] is presented in Fig. 1. The total crushing force in inertial crusher is sum of centrifugal forces developed by unbalance centrifugal vibrator F_{ucv} (N) and inner cone F_{ic} (N). The first approximation in calculation process is neglecting the components of transverse movement cone precession so that is possible to calculate centrifugal forces by classical formula:

$$F_{cent} = m.e.\omega_i^2, \quad N \quad (1)$$

As follows that simplification the oscillations of the inner cone could be represented by its precession

movement around the spherical bearing center. It is possible to describe with acceptance of [4], centrifugal force generated by the oscillating motion of the inner cone:

$$F_{ic} = m_{ic} \cdot e_1 \cdot \omega_{icp}^2, \quad N \quad (2)$$

and the centrifugal force generated by the rotation of the unbalance vibrator:

$$F_{ucv} = m_{cv} \cdot e \cdot \omega_{cv}^2, \quad N \quad (3)$$

where: m_{ic} (kg) – inner cone mass; m_{cv} (kg) – centrifugal vibrator mass; e_1 (m) – eccentricity (distance) from precession axis of inner cone to its mass center; e (m) – eccentricity (distance) from rotation axis of centrifugal vibrator to its mass center; ω_{icp} (rad/s) – angular speed of inner cone precession; ω_{cv} (rad/s) – angular speed of centrifugal vibrator.

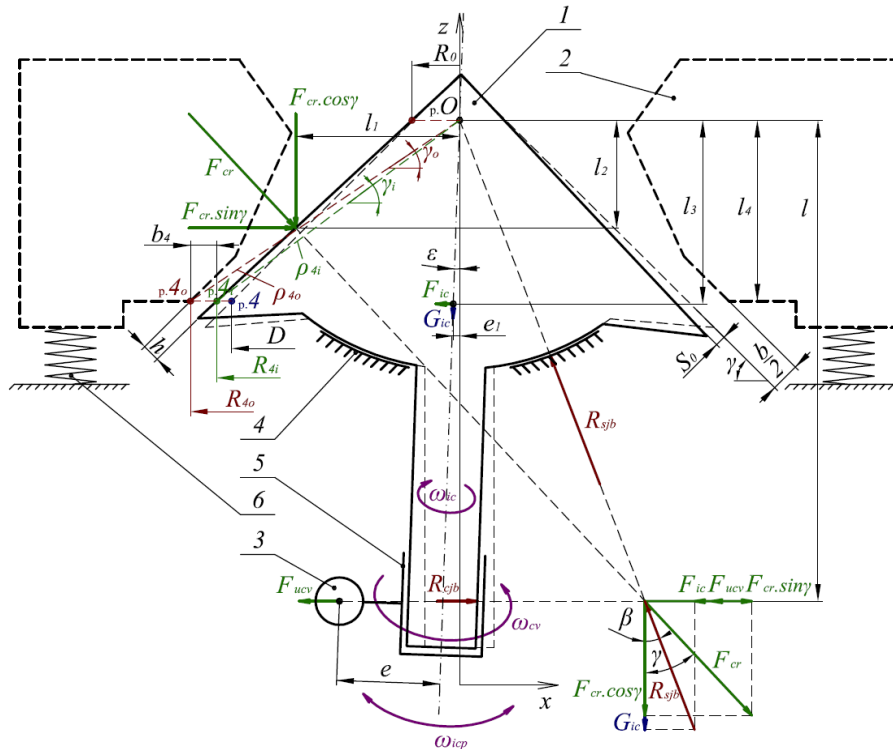


Fig. 1. Force and speed layout of the inner cone.

According to [1, 2] resulting crushing force, render the fact the crusher is mounted on elastic elements can be determined with accounting force transfer loosing [1, 2]. Hence v_{ic} and v_{ucv} are force transfer loosing coefficients rendering that there is no ideal way to transmit force from one body to another. Valuable it is equal to one (100 %) for absolutely stationary housing (outer cone) or it is less than one (100 %) in housing mounted on the elastic elements, so they can be calculated as:

$$v_{ic} = \frac{I_h \cdot I_{ic} \cdot m_{cr} - I_h \cdot S_{ic}^2 - I_{ic} \cdot S_h^2}{I_{ic} \cdot (I_{cr} \cdot m_{cr} - S_{cr}^2)} \quad (4)$$

$$v_{ucv} = \frac{S_h \cdot (I_{ic} - S_{cr} \cdot l) - I_h \cdot (S_{ic} - m_{cr} \cdot l)}{l \cdot (I_{cr} \cdot m_{cr} - S_{cr}^2)} \quad (5)$$

where: I_{cr} , I_h , I_{ic} (kg.m²) – central inertia moments of the crusher, the housing and the inner cone; S_{cr} , S_h , S_{ic} (kg.m) – central mass static moments of the crusher, the housing and the inner cone; m_{cr} (kg) – crusher mass; l (m) – distance between spherical bearing center and rotation plane of vibrator mass center.

Crushing force can be calculated as follows with accounting the distances and their change from application points of the forces generated by

unbalance vibrator and inner cone, to the center of the spherical bearing, ignoring the angle of precession small components of the total crushing force:

$$F_{cr} = \frac{l_3 \cdot v_{ic} \cdot F_{ic} + l_4 \cdot v_{ucv} \cdot F_{ucv}}{l_1 \cdot \cos \gamma + l_2 \cdot \sin \gamma}, \quad N$$

$$F_{cr} = F'_{ic} + F'_{ucv}, \quad N \quad (6)$$

where: l_1 (m) – X distance between crushing force application point and center of spherical bearing; l_2 (m) – Z distance between crushing force application point and center of spherical bearing; l_3 (m) – Z distance between inner cone force (mass center of inner cone) and center of spherical bearing; l_4 (m) – distance between center of spherical bearing and edge of outer cone and component forces F'_{ic} (N) and F'_{ucv} (N) are described below.

Distances changes come in calculation due to crushing chamber area and volume change depending to the static discharge hole adjustment which results are shown in table 2 It is used the dependence of curvilinear polygon area formed by the sides of the cones (application point is the center of gravity of the geometrical shape of the diagram of the distributed loads along the lining of the inner cone (rectangular trapezoid with curved thigh) as follows:

$$A_{ch}(l, b) = A_{ch_0} + l_4(b) \cdot 0,5 \cdot b, \quad m^2 \Rightarrow$$

$$A_{ch}(l, b) = A_{ch_0} + A_{ch_1} \cdot b, \quad m^2 \quad (7)$$

The distances l_1 (m) and l_2 (m) dependences are represented as:

$$l_1 = l_1(b), \quad m \quad ; \quad l_2 = l_2(b), \quad m \quad (8)$$

Hence the description of geometrical connections in the crushing chamber is represented in the subsequent equations with acceptance of idealizations and dimensions shown on Fig. 1, as follows: R_0 (m) – cone radius at horizontal plane section at center of spherical movement $p.O$; D (m) – cone diameter at horizontal plane section at discharge point $p.4$ ($p.4_i$ is a projection of discharge (plane) line over an inner cone and $p.4_o$ is a projection of discharge (plane) line over an outer cone); γ (rad) – cone generant (side) angle; γ_i (rad) – angle between inner generant line $O4_i$ and horizontal axis; γ_o (rad) – angle between outer generant line $O4_o$ and horizontal axis.

Horizontal projection (hypotenuse) of crusher static discharge is:

$$b_4 = \frac{b}{2 \cdot \sin \gamma}, \quad m \quad (9)$$

Radius from outer cone axis to inner projection $p.4_i$ is:

$$R_{4_i} = \frac{l_4}{\tan \gamma} + R_0, \quad m \quad (10)$$

Radius from outer cone axis to outer projection $p.4_o$ is:

$$R_{4_o} = R_{4_i} + b_4 = \frac{l_4}{\tan \gamma} + R_0 + b_4 =$$

$$= \frac{l_4}{\tan \gamma} + R_0 + \frac{b}{2 \cdot \sin \gamma}, \quad m \quad (11)$$

Inner generant angle is:

$$\tan \gamma_i = \frac{l_4}{R_{4_i}} = \frac{l_4 \cdot \tan \gamma}{l_4 + R_0 \cdot \tan \gamma} \Rightarrow$$

$$\gamma_i = \arctan \left[\frac{l_4 \cdot \tan \gamma}{l_4 + R_0 \cdot \tan \gamma} \right], \quad rad \quad (12)$$

Outer generant angle is:

$$\tan \gamma_o = \frac{l_4}{R_{4_o}} = \frac{l_4 \cdot \tan \gamma}{l_4 + (R_0 + b_4) \cdot \tan \gamma} \Rightarrow$$

$$\gamma_o = \arctan \left[\frac{l_4 \cdot \tan \gamma}{l_4 + (R_0 + b_4) \cdot \tan \gamma} \right], \quad rad \quad (13)$$

Radius of spherical movement of inner projection point, a distance between $p.O$ to $p.4_i$ is:

$$\rho_{4_i} = \frac{l_4}{\sin \gamma_i}, \quad m \quad (14)$$

Radius of spherical movement of outer projection point, a distance between $p.O$ to $p.4_o$ is:

$$\rho_{4_o} = \frac{l_4}{\sin \gamma_o}, \quad m \quad (15)$$

Those data and these geometrical dependencies form the minimum necessity parameters used in calculation of the inner cone precession angle as:

$$\varepsilon = \frac{\hat{S}_0}{\rho_{4_i}} \Rightarrow \varepsilon \approx \frac{S_0 \cdot \sin \gamma_i}{l_4}, \quad rad \quad (16)$$

The crusher dynamical discharge value is:

$$h = \frac{1}{2} \cdot b - S_0, \quad m \Rightarrow h = \frac{1}{2} \cdot b - \frac{\varepsilon \cdot l_4}{\sin \gamma_i}, \quad m \quad (17)$$

The eccentricity value of inner cone movement is limited by the cone sides touching so it's maximal value e_1^{max} (m) means that dynamical discharge h (m) is zero. The formulation of inner cone eccentricity is:

$$\hat{e}_1 = \varepsilon \cdot l_3, \quad m \Rightarrow e_1 = \varepsilon \cdot l_3, \quad m \Rightarrow$$

$$e_1 = S_0 \cdot \sin \gamma_i \cdot \frac{l_3}{l_4}, \quad m \quad (18)$$

The connection between geometrical parameters of machine and technological parameters came through the connection of dynamical discharge hole h (m) average value \bar{h} (m). With some assumptions and probabilities analysis the particle output from discharge hole can be averaged as particle size mean diameter, so:

$$\bar{h} = d_{0_{av}}, \quad m \quad (19)$$

This will allow expressing the averaged dynamical movement of inner cone as:

$$\bar{S}_0 = \frac{1}{2} \cdot b - d_{0_{av}}, \quad m \quad (20)$$

III. FORCE CREATION AND DEPENDENCIES

Force dependencies and relationships between those created from inner cone and unbalanced vibrator study and their sum in the total crushing force. The upper equations and some geometry information taken from 3D CAD model are numerically represented in table 1. Some constructive geometrical parameters are respectively: $\gamma=40$ deg; $D=0.3$ m; $l=0.374$ m and $l_3=0.162$ m. The coordinates of the application point of the resultant crushing force (distances l_1 (m) and l_2 (m)) and e_1 (m) are dependent on the static discharge opening width b (m). The eccentricity value e (m) is determined by the size of the mass moment of static unbalance vibrator (his degree). Based on the above of (4) and (5) are defined the coefficients $v_{ucv}=0.982$ and $v_{ic}=0.977$.

Forces generated by unbalance vibrator and inner cone can be determined from the following equations:

$$F'_{ucv} = \frac{v_{ucv} \cdot m_{cv} \cdot e \cdot l \cdot \omega_{cv}^2}{l_1 \cdot \cos \gamma + l_2 \cdot \sin \gamma}, \quad N \quad (21)$$

$$F'_{ic} = \frac{v_{ic} \cdot m_{ic} \cdot e_1 \cdot l_3 \cdot \omega_{icp}^2}{l_1 \cdot \cos \gamma + l_2 \cdot \sin \gamma}, \quad N \quad (22)$$

The angular velocity of the unbalance vibrator ω_{cv} (rad/s) is determined by the gear ratio of the V-belt transmission and the rotation frequency of the drive motor. Due to the lack of rigid kinematic connection between the drive system and the inner cone the frequency of precession of the inner cone ω_{icp} (rad/s) is quite complicated to be determined theoretically.

According to previous researchers [1, 2, 3] frequency of precession (oscillation) of the inner cone is 30 to 100 times lower than the frequency of rotation of the unbalance vibrator based on the size and the settings of the machine and depending on the condition and the physical and mechanical characteristics of crushed material. On this basis it is introduced a coefficient of proportionality:

$$k_p = \frac{n_{cv}}{n_{icp}} = \frac{\omega_{cv}}{\omega_{icp}} \quad \therefore \quad k_p = 30 \div 100 \quad (23)$$

and it is obtained:

$$F'_{ic} = \frac{v_{ic} \cdot m_{ic} \cdot e_1 \cdot l_3 \cdot \omega_{cv}^2}{k_p^2 \cdot (l_1 \cdot \cos \gamma + l_2 \cdot \sin \gamma)}, \quad N \quad (24)$$

The variables values in (21), (22) and (24) are determined through CAD model and some calculations, so the results are represented in table 2 for a particular value for $k_p=30$. Therefore the force values developed by the unbalance vibrator are calculated in various settings of the crusher.

In (24) all parameters are determined numerically with the exception of the proportionality factor k_p . The magnitude of the force generated by the inner cone can be determined only with known value or functional dependence of the proportionality factor k_p . In order to study what part (share) of the total force of crushing is the force generated by the inner cone (when the machine operating with different settings and with different values of k_p), the forces generated by unbalance vibrator and the inner cone are presented as a relative force, using the following equations:

$$F'_{ucv,\%} = \frac{F'_{ucv}(N)}{F_{cr}(N)} \cdot 100, \quad \%; \quad F'_{ic,\%} = \frac{F'_{ic}(N)}{F_{cr}(N)} \cdot 100, \quad \% \quad (25)$$

Results for the value of the force generated by the inner cone are presented in table 3, as a percentage of the total crushing force, obtained in different settings of the crusher and a variable coefficient of proportionality k_p in the range $1 \div 100$.

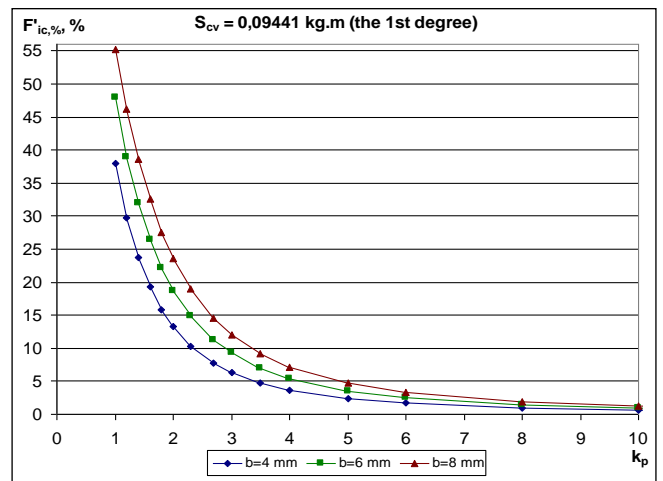


Fig. 2. $F'_{ic,\%}=f(k_p)$ at $b=4, 6$ and 8 mm and a minimum degree of unbalance vibrator.

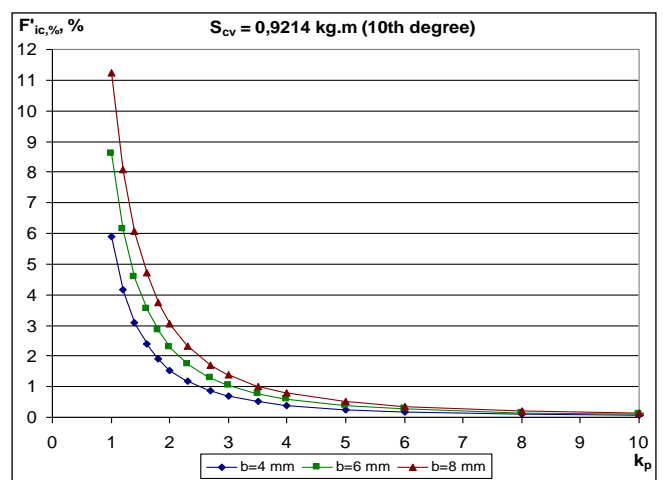


Fig. 3. $F'_{ic,\%}=f(k_p)$ at $b=4, 6$ and 8 mm and an average degree of unbalance vibrator.

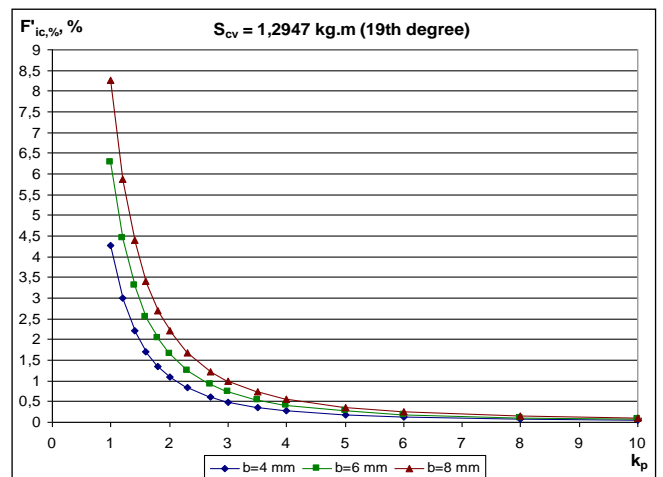


Fig. 4. $F'_{ic,\%}=f(k_p)$ at $b=4, 6$ and 8 mm and a maximum degree of unbalance vibrator.

Based on the results obtained are presented few graphical (Fig. 2, 3 and 4) dependencies of the partition of the inner cone force (in relative units) dependence to the coefficient of proportionality, respectively, in different static discharge opening width $b=4, 6$ and 8 mm and at a minimum (the 1st) average (10th) and maximum (19th) degree of unbalance vibrator.

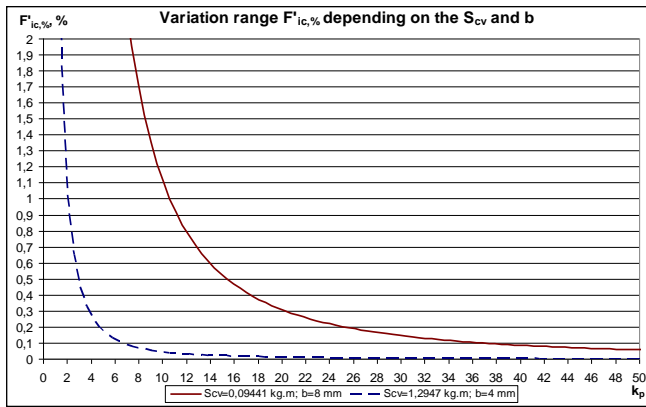


Fig. 5. The range of variation of the share of force generated by the inner cone presented in relative units (in percent of the total force of crushing).

Figure 5 presents the range of variation in the share of force generated by the inner cone, as a percentage of the total force of crushing, depending on the mass static moment of unbalance vibrator and the static discharge opening width.

Equations 21, 22 and 24 gave a complicated dependence clearly presented in graph results shown in Fig. 2, 3, 4 and 5. Hence it is done a few mathematical preparations and simplification, as it is expressed in following steps the equation for relative inner cone force:

$$F'_{ic} = \frac{F'_{ic}}{F'_{ucv}} = \frac{v_{ic} \cdot m_{ic} \cdot e_1 \cdot J_3}{k_p^2 \cdot v_{ucv} \cdot m_{cv} \cdot e \cdot l} = \frac{v_{ic} \cdot m_{ic} \cdot J_3}{v_{ucv} \cdot m_{cv} \cdot e \cdot l} \cdot \frac{e_1}{k_p^2}$$

$$F'_{ic} = k_{mg} \cdot \frac{e_1}{k_p^2} \quad (26)$$

It was explained that there is a complicated functional connection between e_1 (m) and J_3 (m) and geometrical parameter b (m), dynamical F_{cr} (N) and technological parameters S_0 (m), so there is a variables split shown in (26). After an application of (18) in (26), it is obtained:

$$F'_{ic} = \frac{F'_{ic}}{F'_{ucv}} = \frac{v_{ic} \cdot m_{ic} \cdot J_3^2}{v_{ucv} \cdot m_{cv} \cdot e \cdot l \cdot J_4} \cdot \frac{S_0}{k_p^2}$$

$$F'_{ic} = k_{mgt} \cdot \frac{S_0}{k_p^2} \quad (27)$$

Those relations are represented Fig. 6, with a certain acceptance that less 2 % influence of inner cone force over centrifugal vibrator force is insignificant and possible to be neglected. Comparison between this functional research (Fig. 6 and (26), (27), (28)) and calculation (Fig. 2, 3, 4, 5, table 2 and (21), (22), (24), (25)) is quite similar.

The derivative function used for investigation of relative inner cone force sensibility to geometry, dynamic and technological parameters and it is calculated as:

$$\frac{dF'_{ic}}{dk_p} = -2 \cdot k_{mg} \cdot \frac{e_1}{k_p^3} \quad (28)$$

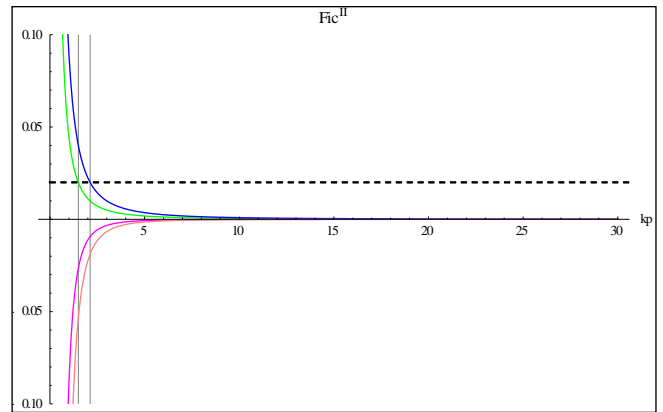


Fig. 6. Relative inner cone force (green, blue) and its derivative function (magenta, pink) from k_p value. Grid line show 2 % limit. Blue line shows relative inner cone force for maximal value of e_1 (m) and green line for its minimal value.

IV. CONCLUSIONS

Results from calculation and represented diagrams shown in Fig. 2, 3 and 4 for the proportion of inner cone force, as a percentage to total crushing force increases in the following cases:

- When reducing the value of the proportionality factor.
- When reducing of degree of the unbalance vibrator.
- When increasing the static discharge opening width.

From Fig. 2 it is seen that the inner cone force up to a maximum of 55 % in the static discharge opening width $b=8$ mm and $k_p=1$ at the theoretical formulation of equality by the vibrator angular speed and angular speed of cone precession. The kinematics scheme of any real construction of cone inertial crusher, especially type KID, can not provide such a coincidence of those two parameters. From Fig. 5 it is seen that regardless of the settings of the crusher when a coefficient of proportionality is greater than 8, the share of the inner cone force is less than 1.9 % of the total force of crushing, and for the range in which a crusher works ($k_p \geq 30$) the share of the force generated by the inner cone is below 0.14 % of the total force of crushing.

An analytical study shows that the force generated by the inner cone is not a significant factor at crushing of the material in cone inertial crushers type KID-300. Due to the negligible amount of force (compared to a total force of crushing) it can be ignored for various idealizations in the dynamic modeling. The factor which determined the crushing process is the force generated by the unbalance vibrator. The sensitivity of centrifugal vibrator force to the inner cone force is non significant (less than 2 %) in applications with $k_p > 2,2$.

REFERENCES

- [1] V. Arsentiev, L. Vaisberg, L. Zarogatsky and A. Shuloyakov, Production of Cubiform Crushed Stone and Road Construction Sand through the Use of Vibratory Crushers,

- VSEGEI, Saint-Peterburg, 2004 (Text in Russian)
- [2] L. Vaisberg, L. Zarogatsky and V. Turkin, Vibratory Crushers, VSEGEI, Saint-Peterburg, 2004 (Text in Russian)
- [3] L. Zarogatsky, "Application of inertial crushers in processing of diamond raw materials", Obogashchenie Rud, 1993, No. 5-6 (Text in Russian)
- [4] Yu. Muzemnek, G. Kalyunov and E. Kochetov, Cone Crushers, Mashinostroene, Moscow, 1970 (Text in Russian)
- [5] S. Savov, "Constructive-mechanical review of conical inertial crushers (KID)", Bulgarian Journal for Engineering Design, September 2012, No. 15, pp. 23-28, ISSN 1313-7530 (Text in Bulgarian)
- [6] S. Sergeev and R. Zakirov, "Inertial rotary vibrational drives for crushers of brittle materials", Russian Engineering Research, 2012, Vol. 32, No. 2 (Text in Russian)
- [7] <http://www.wolfram.com/mathematica/>

APPENDIX

TABLE I. INERTIAL PARAMETERS OF KID-300 AND ITS NODES

Node	Mass, kg	Overall dimensions $x; y; z$, mm	Mass static moment S_z , kg.m	Moments of inertia, kg.m ²		
				I_x	I_y	I_z
Crusher	838,616	790x946x902	120,305	61,44022	61,44005	51,5163
Housing and outer cone	701,327	790x946x854	113,377	56,774	56,773	50,342
Inner cone	79,941	375x375x464	4,4287	0,98218	0,98219	0,7687
Unbalance vibrator						
minimum degree	43,147	305x300x239	0,0944	0,27703	0,37433	0,3872
average degree	43,147	305x300x239	0,9214	0,32199	0,32937	0,3872
maximum degree	43,147	305x300x239	1,2947	0,27703	0,37433	0,3872
Cardan shaft	2,738	100x100x191	0,03275	0,009965	0,009965	0,001133
A support unit (rotating part)	11,463	160x160x260	0,29734	0,07709	0,07708	0,02254
Pulley-guided	12,978	220x220x145	0,601	0,0565	0,0565	0,078044
Pulley-leading						
$D_p=156$ mm	5,618	150x150x90	0,1745	0,009808	0,009807	0,014665
$D_p=208$ mm	10,749	220x220x97	0,5074	0,038757	0,038758	0,066632
$D_p=260$ mm	17,826	280x280x113	0,9617	0,07829	0,07788	0,14236
$D_p=300$ mm	16,64	300x300x99	1,074	0,101635	0,101634	0,19605
Motor* (rotor)	95*	350x350x516	–	–	–	(0,045)

TABLE II. THEORETICAL AND EXPERIMENTAL RESULTS $K_p=30$

Nº	b , mm	d_{bas} mm	S_{cv} , kg.m	e , m	ω_{cv} rad/s	F_{ncv} N	e_s , m	ω_{icp} rad/s	F_{ics} N	I_1 , m	I_2 , m	F_{cv} N	F'_{ncv} N	F'_{ics} N	F'_{ncv} in % of F_{cv}	F'_{ics} in % of F_{mp}
1	4	0,538	1,295	0,03001	111,95	15933	0,00168	3,73	1,82	0,117	0,080	42301	42299	2,10	99,995046	0,004954
2	6	0,614	1,295	0,03001	111,53	15814	0,00252	3,72	2,72	0,116	0,080	42142	42138	3,14	99,992547	0,007453
3	8	0,644	1,295	0,03001	111,21	15725	0,00338	3,71	3,63	0,116	0,079	42063	42059	4,20	99,990004	0,009996
4	4	0,635	0,921	0,02135	111,84	11317	0,00168	3,73	1,82	0,117	0,080	30047	30045	2,09	99,993039	0,006961
5	8	0,808	0,921	0,02135	111,42	11233	0,00338	3,71	3,64	0,116	0,079	30048	30043	4,22	99,985954	0,014046
6	6	2,150	0,094	0,00219	112,05	1164	0,00252	3,74	2,75	0,116	0,080	3105	3101	3,17	99,897889	0,102111
7	8	0,000	0,094	0,00219	112,15	1166	0,00338	0,00	0,00	0,116	0,079	3119	3119	0,00	100,000000	0,000000
8	7	0,442	0,921	0,02135	153,83	21411	0,00295	5,13	6,06	0,116	0,079	57167	57160	7,01	99,987741	0,012259
9	6	0,414	0,921	0,02135	153,94	21440	0,00252	5,13	5,18	0,116	0,080	57137	57131	5,98	99,989528	0,010472
10	6	0,451	0,921	0,02135	154,04	21470	0,00252	5,13	5,19	0,116	0,080	57215	57209	5,99	99,989528	0,010472
11	6	0,506	0,921	0,02135	154,04	21470	0,00252	5,13	5,19	0,116	0,080	57215	57209	5,99	99,989528	0,010472
12	6	0,426	0,921	0,02135	154,04	21470	0,00252	5,13	5,19	0,116	0,080	57215	57209	5,99	99,989528	0,010472
13	6	0,448	0,921	0,02135	154,15	21499	0,00252	5,14	5,20	0,116	0,080	57292	57286	6,00	99,989528	0,010472
14	6	0,450	0,921	0,02135	154,15	21499	0,00252	5,14	5,20	0,116	0,080	57292	57286	6,00	99,989528	0,010472
15	6	0,485	0,921	0,02135	154,25	21528	0,00252	5,14	5,20	0,116	0,080	57370	57364	6,01	99,989528	0,010472
16	4	1,254	0,094	0,00219	155,72	2248	0,00168	5,19	3,52	0,117	0,080	5972	5968	4,05	99,932105	0,067895
17	6	1,992	0,094	0,00219	155,72	2248	0,00252	5,19	5,30	0,116	0,080	5996	5990	6,12	99,897889	0,102111
18	8	3,013	0,094	0,00219	155,72	2248	0,00338	5,19	7,11	0,116	0,079	6021	6013	8,24	99,863089	0,136911
19	6	0,460	1,295	0,03001	153,21	29842	0,00252	5,11	5,13	0,116	0,080	79524	79518	5,93	99,992547	0,007453
20	8	0,460	1,295	0,03001	153,31	29883	0,00338	5,11	6,89	0,116	0,079	79935	79927	7,99	99,990004	0,009996
21	4	0,410	1,295	0,03001	154,36	30293	0,00168	5,15	3,46	0,117	0,080	80425	80421	3,98	99,995046	0,004954
22	4	1,371	0,094	0,00219	194,15	3495	0,00168	6,47	5,48	0,117	0,080	9284	9277	6,30	99,932105	0,067895
23	4	1,295	0,094	0,00219	194,15	3495	0,00168	6,47	5,48	0,117	0,080	9284	9277	6,30	99,932105	0,067895
24	6	2,317	0,094	0,00219	194,36	3502	0,00252	6,48	8,26	0,116	0,080	9341	9332	9,54	99,897889	0,102111
25	8	4,012	0,094	0,00219	194,26	3498	0,00338	6,48	11,07	0,116	0,079	9370	9357	12,83	99,863089	0,136911
26	4	0,470	0,921	0,02135	191,53	33191	0,00168	6,38	5,33	0,117	0,080	88123	88117	6,13	99,993039	0,006961
27	6	0,494	0,921	0,02135	190,80	32938	0,00252	6,36	7,96	0,116	0,080	87777	87767	9,19	99,989528	0,010472
28	8	0,537	0,921	0,02135	188,70	32219	0,00338	6,29	10,44	0,116	0,079	86186	86174	12,11	99,985954	0,014046
29	4	0,403	1,295	0,03001	189,86	45829	0,00168	6,33	5,24	0,117	0,080	121673	121666	6,03	99,995046	0,004954
30	6	0,500	1,295	0,03001	188,81	45325	0,00252	6,29	7,80	0,116	0,080	120782	120773	9,00	99,992547	0,007453
31	6	0,469	1,295	0,03001	188,29	45073	0,00252	6,28	7,75	0,116	0,080	120113	120104	8,95	99,992547	0,007453
32	8	0,434	1,295	0,03001	187,55	44723	0,00338	6,25	10,32	0,116	0,079	119631	119619	11,96	99,990004	0,009996
33	4	0,992	0,094	0,00219	225,67	4721	0,00168	7,52	7,40	0,117	0,080	12543	12534	8,52	99,932105	0,067895
34	4	1,047	0,094	0,00219	225,36	4708	0,00168	7,51	7,38	0,117	0,080	12508	12499	8,49	99,932105	0,067895
35	6	2,160	0,094	0,00219	225,88	4730	0,00252	7,53	11,16	0,116	0,080	12617	12604	12,88	99,897889	0,102111
36	8	3,086	0,094	0,00219	226,09	4739	0,00338	7,54	14,99	0,116	0,079	12692	12675	17,38	99,863089	0,136911
37	4	0,306	0,921	0,02135	220,96	44174	0,00168	7,37	7,10	0,117	0,080	117281	117273	8,16	99,993039	0,006961
38	6	0,344	1,290	0,02990	216,25	59248	0,00252	7,21	10,23	0,116	0,080	157886	157874	11,81	99,992521	0,007479
39	8	0,577	1,290	0,02990	211,85	56862	0,00338	7,06	13,16	0,116	0,079	152103	152087	15,26	99,989970	0,010030
40	4	0,414	1,290	0,02990	215,83	59019	0,00168	7,19	6,77	0,117	0,080	156691	156684	7,79	99,995029	0,004971

TABLE III. FORCE GENERATED BY THE INNER CONE

k_p	F'_{ic} in % of F_{cr}								
	$S_{cv}=0,09441$ kg.m			$S_{cv}=0,9214$ kg.m			$S_{cv}=1,2947$ kg.m		
	$b=4$ mm	$b=6$ mm	$b=8$ mm	$b=4$ mm	$b=6$ mm	$b=8$ mm	$b=4$ mm	$b=6$ mm	$b=8$ mm
1	37,9448	47,9150	55,2350	5,8959	8,6140	11,2238	4,2683	6,2862	8,2544
1,2	29,8064	38,9815	46,1458	4,1695	6,1437	8,0711	3,0033	4,4509	5,8805
1,4	23,7789	31,9430	38,6328	3,0976	4,5885	6,0595	2,2242	3,3091	4,3889
1,6	19,2803	26,4355	32,5230	2,3889	3,5513	4,7062	1,7118	2,5534	3,3952
1,8	15,8762	22,1143	27,5798	1,8971	2,8270	3,7556	1,3574	2,0283	2,7018
2	13,2597	18,6982	23,5750	1,5422	2,3022	3,0639	1,1024	1,6493	2,1998
2,3	10,3613	14,8140	18,9134	1,1705	1,7507	2,3342	0,8358	1,2521	1,6723
2,7	7,7387	11,2052	14,4756	0,8521	1,2765	1,7047	0,6079	0,9118	1,2191
3	6,3619	9,2736	12,0569	0,6913	1,0365	1,3853	0,4930	0,7398	0,9898
3,5	4,7543	6,9851	9,1508	0,5089	0,7636	1,0215	0,3626	0,5446	0,7291
4	3,6810	5,4370	7,1597	0,3901	0,5857	0,7840	0,2779	0,4175	0,5592
5	2,3875	3,5492	4,7034	0,2500	0,3756	0,5032	0,1780	0,2676	0,3586
6	1,6702	2,4917	3,3139	0,1737	0,2611	0,3500	0,1237	0,1860	0,2493
8	0,9464	1,4170	1,8915	0,0978	0,1471	0,1972	0,0696	0,1047	0,1404
10	0,6078	0,9116	1,2188	0,0626	0,0942	0,1263	0,0446	0,0670	0,0899
12	0,4228	0,6348	0,8496	0,0435	0,0654	0,0877	0,0310	0,0466	0,0624
16	0,2383	0,3581	0,4797	0,0245	0,0368	0,0494	0,0174	0,0262	0,0351
20	0,1526	0,2295	0,3075	0,0157	0,0236	0,0316	0,0111	0,0168	0,0225
25	0,0977	0,1470	0,1970	0,0100	0,0151	0,0202	0,0071	0,0107	0,0144
30	0,0679	0,1021	0,1369	0,0070	0,0105	0,0140	0,0050	0,0075	0,0100
50	0,0245	0,0368	0,0493	0,0025	0,0038	0,0051	0,0018	0,0027	0,0036
100	0,0061	0,0092	0,0123	0,0006	0,0009	0,0013	0,0004	0,0007	0,0009